AIP Journal of Applied Physics

Enhanced damage buildup in C+-implanted GaN film studied by a monoenergetic positron beam

X. F. Li, Z. Q. Chen, C. Liu, H. J. Zhang, and A. Kawasuso

Citation: Journal of Applied Physics **117**, 085706 (2015); doi: 10.1063/1.4913523
View online: http://dx.doi.org/10.1063/1.4913523
View Table of Contents: http://scitation.aip.org/content/aip/journal/jap/117/8?ver=pdfcov
Published by the AIP Publishing

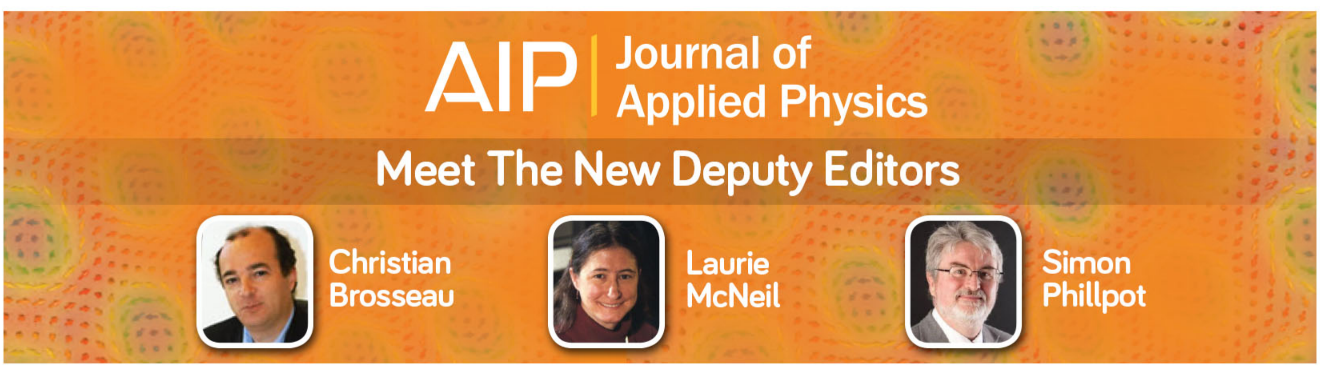

JOURNAL OF APPLIED PHYSICS **117**, 085706 (2015)

Enhanced damage buildup in C^+-implanted GaN film studied by a monoenergetic positron beam

X. F. Li,[1] Z. Q. Chen,[1,a)] C. Liu,[1] H. J. Zhang,[2] and A. Kawasuso[2]
[1]*Department of Physics, Hubei Nuclear Solid Physics Key Laboratory, Wuhan University, Wuhan 430072, China*
[2]*Advanced Science Research Center, Japan Atomic Energy Agency, 1233 Watanuki, Takasaki, Gunma 370-1292, Japan*

(Received 3 December 2014; accepted 13 February 2015; published online 25 February 2015)

Wurtzite GaN films grown by hydride vapor phase epitaxy were implanted with 280 keV C^+ ions to a dose of $6 \times 10^{16}\,\mathrm{cm}^{-2}$. Vacancy-type defects in C^+-implanted GaN were probed using a slow positron beam. The increase of Doppler broadening S parameter to a high value of 1.08–1.09 after implantation indicates introduction of very large vacancy clusters. Post-implantation annealing at temperatures up to 800 °C makes these vacancy clusters to agglomerate into microvoids. The vacancy clusters or microvoids show high thermal stability, and they are only partially removed after annealing up to 1000 °C. The other measurements such as X-ray diffraction, Raman scattering and Photoluminescence all indicate severe damage and even disordered structure induced by C^+-implantation. The disordered lattice shows a partial recovery after annealing above 800 °C. Amorphous regions are observed by high resolution transmission electron microscopy measurement, which directly confirms that amorphization is induced by C^+-implantation. The disordered GaN lattice is possibly due to special feature of carbon impurities, which enhance the damage buildup during implantation. © *2015 AIP Publishing LLC*. [http://dx.doi.org/10.1063/1.4913523]

I. INTRODUCTION

The wide band-gap nitrides have generated significant research interest within the past two decades for both optoelectronic and high-temperature properties. In particular, GaN based blue light-emitting diodes, blue lasers, UV detectors, and microwave power switches have been fabricated, which stimulated extensive investigation on this material.[1–6]

In order to fabricate the above devices, it is necessary to obtain both n-type and p-type conduction in GaN by doping with different impurities. Ion implantation is a very attractive technological tool for doping of GaN. It is one of the important ways for incorporation of dopants in the selected area at controllable amounts. Major progress has been made in the area of p- and n-type doping via implantation in GaN. However, ion implantation makes GaN to be seriously damaged and even becomes amorphous. Post-implantation annealing is necessary to remove undesirable ion-beam damage to make implanted GaN more suitable for device applications. In the previous studies, ion-bombardment-produced defects have been studied in GaN[7–11] and also other group-III nitrides such as InGaN, AlGaN, and AlN.[12,13]

Carbon is a common amphoteric impurity in GaN which affects their technologically important electrical and optical properties. It is reported to contribute p-type conductivity[14] and is expected to be also related to the yellow emission.[15,16] Carbon can be introduced in GaN by several ways such as ion implantation technique. In particular, the presence of a large concentrate of carbon in GaN strongly enhances the accumulation of implantation-produced disorder.[17] This suggests that carbon has special effect which can enhance the damage buildup in GaN. However, in their studies, they used Rutherford backscattering/channeling (RBS/C) spectrometry as the primary method to study the implantation-induced defects and this method is more sensitive to interstitial type defects. Thus, it could not provide more detailed information on the damage accumulation process, such as the introduction and reaction of vacancy defects. Additional method is thus needed to investigate the introduction and recovery process of C^+ implantation-induced defects and probable interaction among these defects.

Positron annihilation spectroscopy (PAS) is a powerful technique to investigate vacancy-type defects in semiconductor materials.[18–21] The positron is particularly sensitive to vacancy-type defects, where the electron density is relatively lower. Because of the reduced electron density and the change of electron momentum distribution at defects, the positron annihilation characteristics such as positron lifetime and Doppler broadening of annihilation radiation at vacancy trapped state are different from the bulk state. Therefore, positron annihilation measurement can provide useful information on the size and concentration of vacancy defects. It will help us to get deeper understand the damage buildup produced by ion implantation.

In this paper, we report our investigations of defect formation and annealing behaviors of C^+-implanted GaN epilayers using positron annihilation spectroscopy together with X-ray diffraction (XRD), Raman scattering, and high resolution transmission electron microscopy (HRTEM). We found that C^+-implantation induces severe damage and cause disordered structure in GaN, which is in contrast to the strong radiation resistance of GaN.

a)Author to whom correspondence should be addressed. Electronic mail: chenzq@whu.edu.cn

II. EXPERIMENT

A ~4 μm thick nominally undoped wurtzite GaN epilayer was grown on (0001) sapphire substrates by hydride vapor phase epitaxy (HVPE). It was purchased from Hefei Kejing Materials Technology, Co., Ltd. The GaN layer was implanted with 280 keV C^+ ions at room temperature with a total dose of $6 \times 10^{16}\,\mathrm{cm}^{-2}$. After implantation, the sample exhibits a much darker color. The post-implantation annealing was carried out from 400 °C to 1000 °C for 30 min in nitrogen ambient at atmospheric pressure.

Defects in the implanted layer were studied using a slow positron beam with positron incident energy ranging from 0.2 keV to 30.2 keV. Doppler broadening of annihilation radiation was measured using a high purity Ge detector with energy resolution of about 1.2 keV at 511 keV. The Doppler broadening spectrum is characterized by the conventional S parameter and W parameter, which is defined as the ratio of the central region ($|P_L| \leq 0.76$ keV) and wing region (3.4 keV $\leq |P_L| \leq 6.8$ keV) to the total area of the 511 keV annihilation peak, respectively. In this paper, all the S parameters and W parameters are normalized to the value in the bulk region of the unimplanted GaN layer. A higher S-parameter (lower W-parameter) than that of the defect-free state is therefore an indication of the existence of vacancy defects.

Lattice structure of GaN layer before and after implantation and annealing was characterized by XRD using a PANalytical diffractometer (Cu Kα radiation). Diffraction pattern is acquired in the 2θ range from 30° to 80° with a step of 0.0167°. Raman scattering (HORIBA Jobin Yvon LabRAM HR, France) was measured at an extended range of 100–1400 cm^{-1} with laser excitation wavelength of 488 nm. Photoluminescence (HORIBA Jobin Yvon LabRAM HR, France) was operated at an extended range of 350–900 nm with laser excitation wavelength of 325 nm. HRTEM (JEOL JEM-2010FEF (UHR), Tokyo, Japan) was performed with acceleration voltage at 200 keV. All the above measurements were performed at room temperature.

III. RESULTS AND DISCUSSION

A. X-ray diffraction

XRD spectra were carried out for the GaN samples before and after C^+-implantation and annealing. The results are shown in Fig. 1. The unimplanted GaN films show good crystallinity of wurtzite structure because the diffraction pattern reveals peaks at about $2\theta = 34.5°$, and 72.8° corresponding to GaN (0002) and (0004) plane. After 280 keV C^+-implantation, a remarkable decreasing of intensity and broadening of the (0002) peak appears. This suggests degradation of the crystal quality after C^+-implantation. Apparently, the GaN lattice structure was severely damaged and may become amorphous after C^+-implantation. Another significant feature of the XRD spectra is that the (0002) peak shifts to lower angles after implantation, which means an expansion of lattice parameters. Generally, the lattice expansion is caused by the incorporation of dopants into material sites or by the occupation of the Ga or N vacancies by larger substituents. Therefore, the shifted peak is, in fact, a damage peak of the GaN (0002).[22]

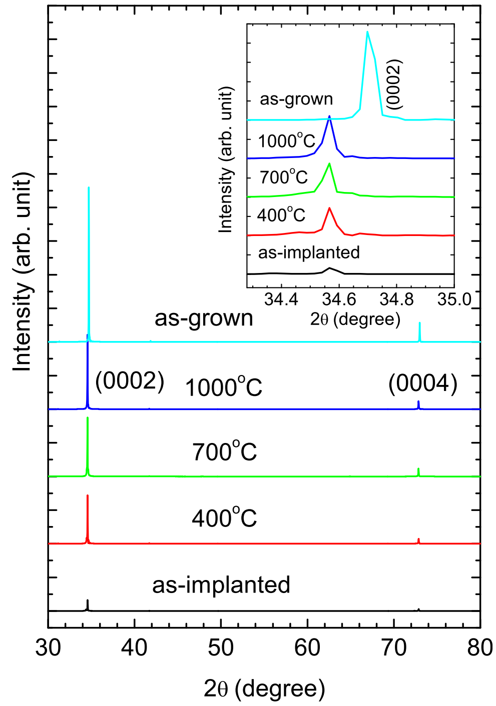

FIG. 1. X-ray diffraction patterns measured for the GaN films before and after C^+-implantation and annealing.

After annealing the implanted sample at 400 °C, the intensity of (0002) peak becomes stronger. Upon increasing up to 1000 °C, the (0002) peak shows a partial recovery. This indicates that the lattice disorder induced by C^+-implantation can be recovered by annealing above 1000 °C. However, annealing process cannot recover the crystal quality to the level of the as-grown GaN films. No other phase related with the implanted C is observed from the XRD pattern in all the samples annealed at different temperatures.

B. Positron annihilation measurements

Figure 2 shows the Doppler broadening S parameter as a function of incident positron energy (S–E curve) measured

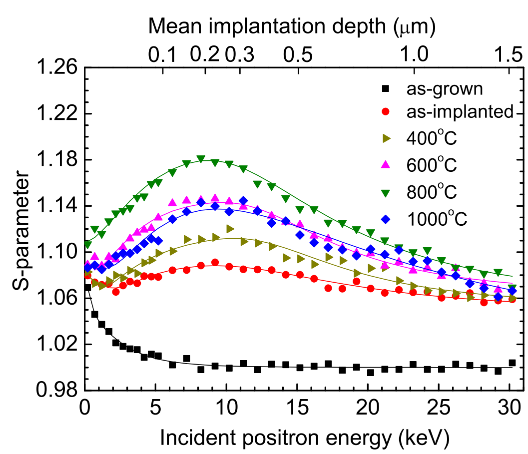

FIG. 2. S–E curve measured for the implanted GaN with dose of $6 \times 10^{16}\,\mathrm{cm}^{-2}$ at different temperature. The solid curves are fits to the experimental data. The annealing was performed in a nitrogen ambient for 30 min. The upper horizontal axis shows the mean implantation depth of positrons for each positron energy.

for the as-grown and C^+-implanted GaN films before and after annealing. The mean implantation depth of positrons is given on the upper axis. In order to avoid overlap of the S–E curves with each other, only some curves at selected annealing temperatures are presented. To check the quality of the as-grown GaN film, we also measured the Doppler broadening spectrum for a GaN single crystal and compared with the unimplanted GaN film in this work. The S-parameters are almost the same for these two samples. In addition, we also measured the positron lifetime of the single crystal GaN sample, which is about 161.3 ps and is close to the bulk lifetime in GaN.[23] We believe that the unimplanted GaN sample is free of vacancy defects, or the concentration of the vacancies is below the detection limit of positrons. Therefore, in this paper, the *S*-parameters are normalized to the value in the as-grown GaN film.

For the unimplanted sample, the *S* parameter decreases gradually with increasing energy and approaches a constant value at energy E $\sim$ 7 keV. This is due to the transition of positron annihilation from the surface state to the bulk state with increasing implantation depth. After C^+-implantation, the *S* values show an overall increase in the whole positron energy range compared with those for the unimplanted sample. This was due to the annihilation of positrons in vacancy-type defects introduced by the ion implantation. The *S* parameter in the positron energy of 6–15 keV for the as-implanted GaN increases to above 1.08, and the peak *S*-parameter is around 1.09. This high *S* parameter range coincides with the 280 keV C^+-implantation profile, which has a stopping range R_P of about 409 nm according to the Monte Carlo simulation program TRIM.

It should be noted that the maximum *S* parameter in the implanted GaN was observed to occur around a depth of 200 nm. However, the damage profile by 280 keV C^+-implantation has a range of about 409 nm. The different depth between ion range and maximum S parameter is due to the broad positron implantation profile and also the positron diffusion. The positron beam is monoenergetic, it does not mean that all the positrons will stop at the same depth. Instead, the positron has an implantation profile which has width of a few hundred nm or more. The higher the positron energy, the broader will be the implantation profile. So, we use the average implantation depth for each positron incident energy. This means that even when the average positron implantation depth is inside the damage layer, some part of positrons will extend to the unimplanted region, where the S parameter is much lower. In addition, when the energetic positron beam loses the energy at the depth end, they can also diffuse to any direction. The typical diffusion length will be several nm or even hundreds of nm which depends on the quality of the material. Therefore, the depth of maximum S parameter is always smaller than the ion implantation depth.

In GaN, the possible positron trapping centers are V_{Ga}, $V_{Ga}V_N$ or larger vacancy clusters. V_N is not an effective positron trapping center.[24] The defect species in the implanted GaN can be estimated from the value of *S* parameter. Uedono *et al.* observed an increase of *S* from 0.4415 to about 0.46–0.47 after implantation of Si^+, O^+, and Be^+ ions with a dose of $8.5 \times 10^{14}\,\mathrm{cm}^{-2}$. This corresponds to a normalized S value of about 1.05, and by using positron lifetime measurements together with theoretical calculation, they confirmed that the positron trapping centers were V_{Ga} or $V_{Ga}V_N$.[24] In our results, the large *S* parameter of 1.08–1.09 suggests that the implantation induced defects are not monovacancies or divacancies, but much larger vacancy clusters.

Figure 3 shows the average *S* parameter in the energy range of 7.2 keV–11.2 keV (the implanted region) as a function of annealing temperature. It can be seen that there are two annealing stages. The *S* parameter in the implanted region first increases up to 1.18, then it begins to decrease after annealing above 800 °C. The extremely large *S* parameter of 1.18 indicates positron annihilation in a very large open space. This suggests that possibly microvoids are formed after annealing the implanted sample. Probably, the positronium may have also formed and annihilate in the microvoids. Since the para-positronium contains nearly zero momentum, its self annihilation will contribute a very narrow peak to the Doppler broadening spectrum, which leads to the substantial increase of *S* parameter. It can be also observed that the positron incident energy corresponding to the maximum *S* parameter shifts to lower value (from 10.2 keV to 8.2 keV) with increasing annealing temperature, suggesting that the damage layer generated by implantation moves towards the surface.

The vacancy clusters and microvoids begin to recover after annealing at temperatures higher than 800 °C. After annealing at 1000 °C, the *S* parameter decreases to about 1.14. This is still much higher than the value for the unimplanted sample, suggesting that the implantation induced defects are difficult to be annealed out. Saarinen *et al.* reported that the electron irradiation induced monovacancies V_{Ga} can be annealed at relatively low temperature of 400–500 K.[25] However, for ion-implanted GaN, the induced extended defects such as vacancy clusters and their related complexes remain stable even after annealing at high temperature of 1300 °C.[24] It is difficult to remove defects induced by implantation in GaN.[26] This is because of the ultra high melting temperature of GaN, which is about 2500 °C. Generally, a temperature of $\sim$2/3 of the melting temperature (in Kelvin) is needed to remove extended

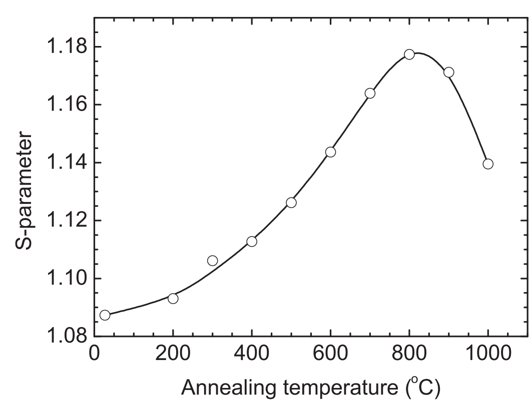

FIG. 3. Average *S* parameter in the energy range of 7.2 keV to 11.2 keV in the implanted region as a function of annealing temperature for ion-implanted GaN.

defects in semiconductors. According to this rule, an annealing temperature higher than 1600 °C is necessary to remove the implantation induced defects in GaN. However, such high temperature annealing will lead to complete decomposition of the near-surface layer. Actually, we have already observed decomposition of GaN even after annealing our sample at 1100 °C. After annealing at 1200 °C, the GaN epilayer disappears completely, and only the information of the sapphire substrate can be obtained from the slow positron beam measurements.

C. Raman scattering measurements

Figure 4 shows the Raman spectra measured for GaN before and after implantation and annealing. For the as-grown sample, there are two phonon modes. The dominant peaks at 568 and 735 cm^{-1} are the E_2 (high) and A_1 (LO) modes, respectively, which are characteristics of the GaN wurtzite crystal structure. This result is consistent with those reported previously.[27–29] There is another weak peak at 144 cm^{-1}, which is the E_2 (low) mode. These peaks are all in accordance with the Raman selection rule for wurtzite crystal structure. After C^+-implantation, the peaks corresponding to E_2 (high) and A_1 (LO) modes become very weak, and the 144 cm^{-1} peak dominates the whole measured range and becomes significantly strong and broad. In other ion-implanted GaN films, such as Ar^+, Mg^+, P^+, and Ca^+, the primary E_2 peaks at 568 and 735 cm^{-1} still exist but become weak,[27] which means that the wurtzite lattice structure of GaN is not destroyed by implantation. However, in our C^+-implanted GaN, all the phonon modes related to GaN disappear. This suggests that the GaN lattice structure is severely damaged and becomes disordered in the implanted layer.

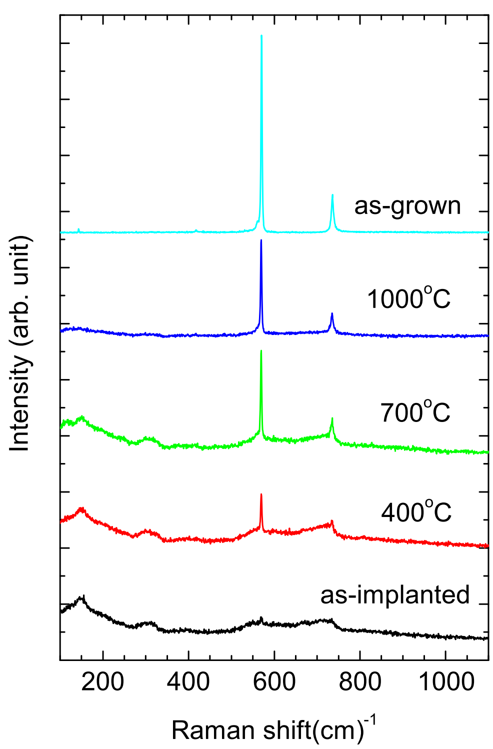

FIG. 4. Raman scattering spectra measured for the GaN before and after C^+-implantation and annealing.

The C^+-implantation in GaN also induces an additional broad peak at around 300 cm^{-1}. This is apparently due to the implantation induced defects, and is not related with the implanted carbon. Limmer *et al.* also observed this peak in several ion-implanted GaN, and they ascribe this peak to the disordered GaN structure induced by implantation. The high dose C^+-implantation in our GaN film would introduce large amounts of defects and cause disorder of the lattice structure, thus breaks the Raman selection rule. Therefore, phonon modes that are forbidden by the selection rule can be observed in the Raman spectrum. This is called the disorder-activated Raman scattering. The broad peak at 300 cm^{-1} is assigned to the highest acoustic-phonon branch at the Brillouin zone boundary.[27]

Annealing the implanted GaN at 400 °C causes appearance of the broad peaks at 568 and 735 cm^{-1}, but the intensity is still weak. After further annealing at 700 °C, the two peaks show a sharp increase and the peak at 144 cm^{-1} shows a decrease. However, the broad peak at 300 cm^{-1} still exists. This indicates that the disordered GaN lattice structure is only partially recovered. With the annealing temperature increasing up to 1000 °C, the 144 cm^{-1} peak shows a sharp decrease. At the same time, the E_2 (high) and A_1 (LO) modes almost reach the same level as the unimplanted sample. The 300 cm^{-1} broad peak also disappears. This suggests that the disordered GaN lattice is almost recovered.

D. Photoluminescence

Photoluminescence spectra for as-grown, C^+-implanted and annealed GaN epitaxial films are shown in Fig. 5. For the unimplanted GaN, there is a dominant near-band-edge UV emission peak located at 3.48 eV with a weak shoulder at 3.28 eV, which were emitted from the large crystallites and emitted from the low angle grain boundaries, respectively.[30,31] The visible light emission at ∼1.7 eV is weak and is probably related with deep level defects.

After C^+-implantation, all the emission bands are completely suppressed, which might be attributable to the poor quality of the implanted GaN lattice structure. This is apparently due to the implantation-induced defects, as some of them act as nonradiative recombination centers. This viewpoint is also supported by the X-ray diffraction, positron annihilation, and Raman scattering measurements. Annealing at temperature below 700 °C has no effect on the measured PL spectra. Further annealing of the implanted sample at 1000 °C still does not lead to the recovery of these emission bands, indicating that most of the nonradiative recombination centers are stable up to 1000 °C. This is in agreement with the defect recovery process revealed by positron annihilation. A large amount of vacancy clusters remain stable even after annealing at 1000 °C. This suggests that the vacancy clusters possibly act as nonradiative recombination centers.

Annealing of the C^+-implanted GaN also causes a weak yellow broad emission centered at around 2.2 eV. As for this

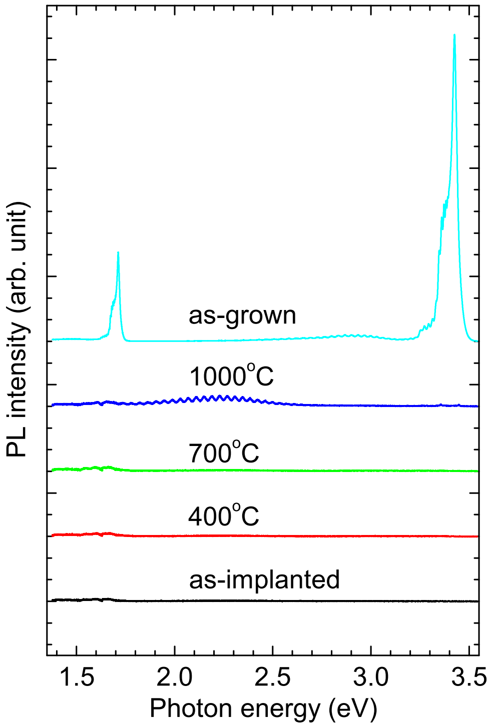

FIG. 5. Photoluminescence spectra measured for the GaN before and after C^+-implantation and annealing.

visible emission bands, its origin is always a difficult problem in GaN. The yellow band has been attributed to Ga vacancies (V_{Ga}) and/or defect complexes composed of V_{Ga} and O.[32,33] It arises because of the Ga vacancies which are formed at high growth temperature with low nitrogen flow rate.[34] Saarinen *et al.* found the linear relationship between the yellow emission intensity and the concentration of V_{Ga}, and concluded that Ga vacancies are associated with the yellow luminescence centers.[35] However, Armitage *et al.* failed to obtain the direct correlation between yellow band and Ga vacancy concentration. Instead, they found a casual relationship between 2.2 eV yellow emission and the carbon impurity, and they proposed a different yellow luminescence mechanism when the carbon impurity concentration is higher than the vacancy concentration.[36] Very recently, Yang *et al.* studied the influence of unintentionally doped carbon impurities on the yellow emission and found that the carbon impurity may preferentially form deep donor complex C_N–O_N resulting from its relatively low formation energy.[4] This complex will induce yellow luminescence in GaN. Other researchers also reported that the yellow emission appeared after annealing was related to complex consisting of C_N.[37]

E. Cross-section HRTEM

To directly understand the microstructure of implanted GaN layer, cross-section HRTEM was performed for the as-implanted GaN film. The obtained images are shown in Fig. 6. It clearly illustrates that the surface morphology notably changes after C^+ implantation. Figure 6(a) shows a cross-sectional (low magnification) TEM image of the GaN film. A surface damage layer with thickness of about 400 nm is found in Fig. 6(a), which coincides with the average ion implantation range from TRIM simulation. An enlarged image of the implanted layer is shown in Fig. 6(b) by increasing the magnification. Some particle-like crystal lattice regions can be observed with almost same orientation, which is obviously the GaN crystal lattice. In the surrounding of those particle-like regions, amorphous structure can be clearly observed. This directly verifies that GaN perfect lattice structure is damaged and amorphous regions are induced by C^+-implantation.

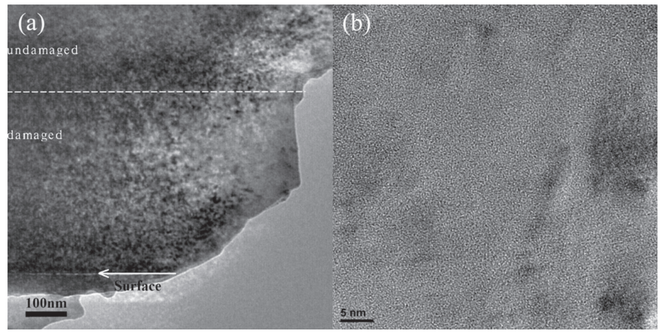

FIG. 6. High resolution transmission electron diffraction images measured for C^+-implanted GaN.

F. Discussion

All the above results suggest that C^+-implantation causes severe damage in GaN. Amorphous regions are also observed clearly by TEM. This could well explain the high Doppler broadening *S* parameter in the as-implanted sample. In the amorphous region, there are numerous large vacancy clusters. Positron annihilating in these vacancy clusters will result in very large S parameters. During post-implantation annealing, these vacancy clusters further grow into microvoids, which is energetically favored process. Therefore a very large *S* parameter of about 1.18 is obtained after annealing at 800 °C.

It is reported that GaN is rather difficult to be amorphized by implantation.[26] This is due to the very efficient dynamic annealing of the defects during ion implantation. Strong recovery of the implantation-induced defects occurs even at liquid nitrogen temperature. However, some particular ion species may enhance the damage buildup during implantation in GaN. For example, the presence of carbon impurities results in a strong enhancement of the buildup of lattice disorder in ion-implanted GaN.[17,38] They can act as effective traps for implantation induced defects and thus enhance the damage buildup. It was further found that this enhanced damage accumulation is due to formation of nitrilelike bonds ($–C \equiv N$),[38] and they stabilize the implantation induced defects.

IV. CONCLUSION

The results of XRD, Raman, and PL all indicate heavy lattice damage induced by C^+-implantation in the GaN films. The disordered lattice structure shows only partial recovery after annealing at high temperature of 1000 °C. Large vacancy clusters are observed in the C^+-implanted region by using a slow positron beam. These vacancy clusters further grow to a larger size or even microvoids after annealing at temperatures up to 800 °C. The amorphous regions observed by HRTEM directly verify that amorphous phase is created by C^+-implantation in GaN films. The severe damage is possibly due to stability of defects by C ions, which enhance the damage buildup during implantation.

ACKNOWLEDGMENTS

This work was supported by the National Natural Science Foundation of China under Grant Nos. 11275143, 11305117, and 11475130.

[1]M. J. Uren, M. Casar, M. A. Gajda, and M. Kuball, Appl. Phys. Lett. **104**, 263505 (2014).
[2]A. Yu. Azarov, A. I. Titov, and S. O. Kucheyev, J. Appl. Phys. **108**, 033505 (2010).
[3]S. O. Kucheyev, H. Timmers, J. Zou, J. S. Williams, C. Jagadish, and G. Li, J. Appl. Phys. **95**, 5360 (2004).
[4]J. Yang, D. G. Zhao, D. S. Jiang, P. Chen, Z. S. Liu, L. C. Le, X. G. He, J. P. Liu, S. M. Zhang, H. Wang, J. J. Zhu, and H. Yang, J. Appl. Phys. **115**, 163704 (2014).
[5]S. O. Kucheyev, J. S. Williams, J. Zou, C. Jagadish, and G. Li, Appl. Phys. Lett. **78**, 1373 (2001).
[6]S. O. Kucheyev, J. S. Williams, A. I. Titov, G. Li, and C. Jagadish, Appl. Phys. Lett. **78**, 2694 (2001).
[7]H. H. Tan, J. S. Williams, J. Zou, D. J. Cockayne, S. J. Pearton, and R. A. Stall, Appl. Phys. Lett. **69**, 2364 (1996).
[8]C. Liu, B. Mensching, M. Zeitler, K. Volz, and B. Rauschenbach, Phys. Rev. B **57**, 2530 (1998).
[9]I. Radu, R. Singh, R. Scholz, U. Gosele, S. Christiansen, G. Bruderl, C. Eichler, and V. Harle, Appl. Phys. Lett. **89**, 031912 (2006).
[10]M. J. Wang, L. Yuan, C. C. Cheng, C. D. Beling, and K. J. Chen, Appl. Phys. Lett. **94**, 061910 (2009).
[11]P. Ruterana, B. Lacroix, and K. Lorenz, J. Appl. Phys. **109**, 013506 (2011).
[12]Jr.-T. Chen, U. Forsberg, and E. Janzen, Appl. Phys. Lett. **102**, 193506 (2013).
[13]A. Uedono, K. Tenjinbayashi, T. Tsutsui, Y. Shimahara, H. Miyake, K. Hiramatsu, N. Oshima, R. Suzuki, and S. Ishibashi, J. Appl. Phys. **111**, 013512 (2012).
[14]H. Przybylinska, G. Kocher, W. Jantsch, D. As, and K. Lischka, AIP Conf. Proc. **772**, 253 (2005).
[15]C. H. Seager, A. F. Wright, J. Yu, and W. Gotz, J. Appl. Phys. **92**, 6553 (2002).
[16]S. O. Kucheyev, M. Toth, M. R. Phillips, J. S. Willians, C. Jagadish, and G. Li, J. Appl. Phys. **91**, 5867 (2002).
[17]S. O. Kucheyev, J. S. Williams, C. Jagadish, J. Zou, G. Li, and A. I. Titov, Phys. Rev. B **64**, 035202 (2001).
[18]M. Jiang, D. D. Wang, Z. Q. Chen, S. Kimura, Y. Yamashita, A. Mori, and A. Uedono, J. Appl. Phys. **113**, 043506 (2013).
[19]Z. Q. Chen, M. Maekawa, A. Kawasuso, R. Suzuki, and T. Ohdaira, Appl. Phys. Lett. **87**, 091910 (2005).
[20]Z. Q. Chen, S. J. Wang, M. Maekawa, A. Kawasuso, H. Naramoto, X. L. Yuan, and T. Sekiguchi, Phys. Rev. B **75**, 245506 (2007).
[21]M. Jiang, X. D. Xue, Z. Q. Chen, Y. D. Liu, H. W. Liang, H. J. Zhang, and A. Kawasuso, J. Mater. Sci. **49**, 1994 (2014).
[22]C. Liu, B. Mensching, K. Volz, and B. Rauschenbach, Appl. Phys. Lett. **71**, 2313 (1997).
[23]S. Hautakangas, J. Oila, M. Alatalo, K. Saarinen, L. Liszkay, D. Seghier, and H. P. Gislason, Phys. Rev. Lett. **90**, 137402 (2003).
[24]A. Uedono, K. Ito, H. Nakamori, K. Mori, Y. Nakano, T. Kachi, S. Ishibashi, T. Ohdaira, and R. Suzuki, J. Appl. Phys. **102**, 084505 (2007).
[25]K. Saarinen, T. Suski, I. Grzegory, and D. C. Look, Phys. Rev. B **64**, 233201 (2001).
[26]S. O. Kucheyev, M. Toth, M. R. Phlilips, J. S. Williams, C. Jagadish, and G. Li, Appl. Phys. Lett. **78**, 34 (2001).
[27]W. Limmer, W. Ritter, R. Sauer, B. Mensching, C. Liu, and B. Rauschenbach, Appl. Phys. Lett. **72**, 2589 (1998).
[28]W. H. Sun, S. T. Wang, J. C. Zhang, K. M. Chen, G. G. Qin, Y. Z. Tong, Z. J. Yang, G. Y. Zhang, Y. M. Pu, Q. L. Zhang, J. Li, J. Y. Lin, and H. X. Jiang, J. Appl. Phys. **88**, 5662 (2000).
[29]W. H. Sun, S. J. Chua, and X. H. Zhang, J. Appl. Phys. **91**, 4917 (2002).
[30]B. J. Pong, C. J. Pan, Y. C. Teng, G. C. Chi, W. H. Li, and K. C. Lee, J. Appl. Phys. **83**, 5992 (1998).
[31]F. A. Ponce, D. P. Bour, W. Gotz, and P. L. Wright, Appl. Phys. Lett. **68**, 57 (1996).
[32]J. Neugebauer and C. G. Van de Walle, Appl. Phys. Lett. **69**, 503 (1996).
[33]M. Kubota, T. Onuma, Y. Ishihara, A. Usui, A. Uedono, and S. F. Chichibu, J. Appl. Phys. **105**, 083542 (2009).
[34]G. Koblluler, F. Reurings, F. Tuomisto, and J. S. Speck, Appl. Phys. Lett. **97**, 191915 (2010).
[35]K. Saarinen, T. Laine, S. Kuisma, J. Nissila, P. Hautojarvi, L. Dobrzynski, J. M. Baranowski, K. Pakula, R. Stepniewski, M. Wojdak, A. Wysmolek, T. Suski, M. Leszczynski, I. Grzegory, and S. Porowski, Phys. Rev. Lett. **79**, 3030 (1997).
[36]R. Armitage, W. Hong, Q. Yang, H. Feick, J. Gebauer, E. R. Weber, S. Hautakangas, and K. Saarinen, Appl. Phys. Lett. **82**, 3457 (2003).
[37]J. L. Lyons, A. Janotti, and C. G. Van de Walle, Appl. Phys. Lett. **97**, 152108 (2010).
[38]S. O. Kucheyev, J. E. Bradby, C. P. Li, S. Ruffell, T. van Buuren, and T. E. Felter, Appl. Phys. Lett. **91**, 261905 (2007).